Supplementary Information:

1. Measurement sequence

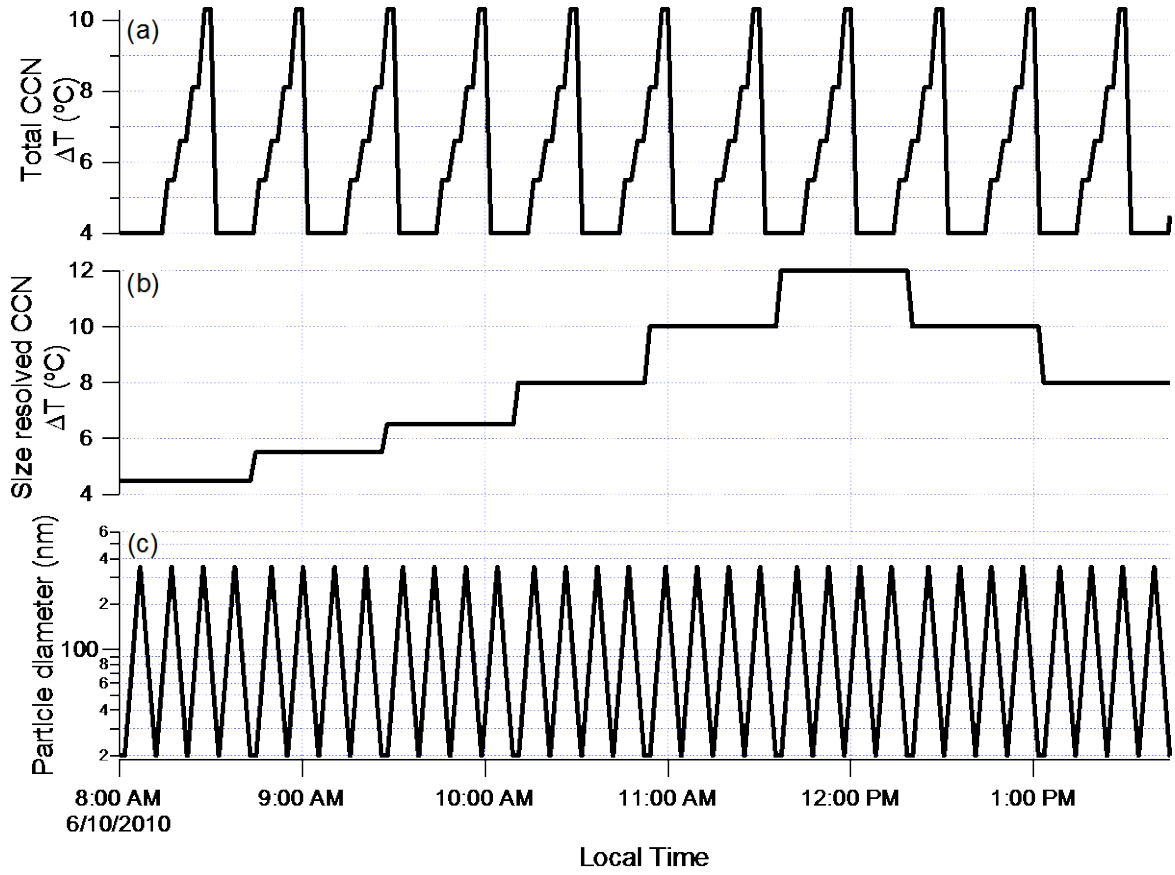

Figure S1. An example of measurement sequences for (a) the CCN counter temperature gradient for total CCN concentration measurements, (b) the CCN counter temperature gradient and (c) the particle size classified by DMA for the size resolved CCN measurements.

2. Derivation of particle hygroscopicity and mixing state

The activated fractions measured at the six supersaturations were fitted using following two different functions (Mei et al., 2012):

$$R_a(S) = \frac{E}{2} \cdot \left(1 + erf\left(\frac{\ln S - \ln S^*}{\sqrt{2\sigma_S{}^2}} \right) \right) \quad \text{(S1)}$$

and (Lance, 2007; Bougiatioti et al., 2011; Cerully et al., 2011; Lance et al., 2012; Padro et al., 2012):

$$R_a(S) = \frac{E}{1 + \left(\frac{S}{S^*} \right)^C} \quad \text{(S2)}$$

The fitting parameters are E, S^*, and σ_S for Eqn. (S1) and E, S^*, and C for Eqn. (S2), where σ_S and C are related to the slope of the increasing R_a with S near S^*. For each set of measurements, the function form that yielded the best fit (i.e. smaller least squares residue) was used for subsequent analysis.

For particles with the same size and composition (i.e., hygroscopicity), we would expect a step function for R_a as all particles would have the identical S_c. Ambient aerosols show much more gradual increase in R_a (i.e., instead of a step change), suggesting heterogeneity in particle S_c. The probability density function (PDF) of the critical supersaturation for size selected particles, $p(S_c)$ is given by differentiating $R_a(S_c)$ with respect to S_c:

$$p(S_c) = \frac{1}{E} \cdot \frac{dR_a(S_c)}{dS_c} \quad \text{(S3)}$$

The dispersion in S_c is defined as $\sigma(S_c)/\overline{S_c}$, where $\overline{S_c}$ is the average particle critical supersaturation:

$$\overline{S_c} = \int_0^\infty p(S_c) \cdot S_c \cdot dS_c \quad \text{(S4)}$$

and

$$\sigma^2(S_c) = \int_0^\infty \left(S_c - \overline{S_c}\right)^2 p(S_c) dS_c \quad \text{(S5)}$$

When $R_a(S)$ is fitted using Eqn. (S1), the hygroscopicity dispersion is:

$$\frac{\sigma(S_c)}{\overline{S_c}} = \left[e^{\sigma_S{}^2} - 1\right]^{1/2} \quad \text{(S6)}$$

and for Eqn (S2), the dispersion is given by:

$$\frac{\sigma(S_c)}{\overline{S_c}} = \left[\frac{\Gamma\left(\frac{2}{C}+1\right)\cdot\Gamma(1-2/C)}{\Gamma(2)} \Bigg/ \left(\frac{\Gamma\left(\frac{1}{C}+1\right)\cdot\Gamma(1-1/C)}{\Gamma(2)} \right)^2 - 1 \right]^{1/2} \quad \text{(S7)}$$

The dispersion in S_c is due to the combination of the width of DMA transfer function (particles classified by DMA do not have exactly the identical size) and the heterogeneity in particle composition (i.e., hygroscopicity), and can be expressed as (Lance et al., 2012):

$$\left(\frac{\sigma(S_c)}{\overline{S_c}}\right)^2 = \frac{9}{4}\left(\frac{\sigma(D_p)}{\overline{D_p}}\right)^2 + \frac{1}{4}\left(\frac{\sigma(\kappa)}{\overline{\kappa}}\right)^2 \quad \text{(S8)}$$

Where the first term on the RHS of the equation represents the contribution due to the width of DMA transfer function, which was estimated from the dispersion in S_c measured during calibration using $(NH_4)_2SO_4$ particles (i.e., the contribution of the second term was essentially zero during calibrations). The dispersion in hygroscopicity for classified ambient particles was then derived by subtracting the contribution of DMA transfer function from the total dispersion in measured critical supersaturation.

3. Uncertainty in derived κ_{org}

The hygroscopicity of organic component can be derived from the CCN hygroscopicity as (Eq. 5 in the main text):

$$\kappa_{org} = \frac{1}{x_{org}}\left(\kappa_{CCN} - \kappa_{NH_4NO_3} x_{NH_4NO_3} - \kappa_{(NH_4)_2SO_4} x_{(NH_4)_2SO_4}\right) \quad \text{(S9)}$$

Given the similar hygroscopicities for $(NH_4)_2SO_4$ and NH_4NO_3, we will combine both species and refer to as the inorganic component of the CCN. The hygroscopicity and volume fraction of the inorganic component are given by:

$$\kappa_{inorg} = \frac{\kappa_{NH_4NO_3} x_{NH_4NO_3} + \kappa_{(NH_4)_2SO_4} x_{(NH_4)_2SO_4}}{x_{NH_4NO_3} + x_{(NH_4)_2SO_4}} \quad \text{(S10)}$$

$$x_{inorg} = x_{NH_4NO_3} + x_{(NH_4)_2SO_4} \quad \text{(S11)}$$

Because $(NH_4)_2SO_4$ and NH_4NO_3 have very similar κ values (0.67 and 0.61, respectively), for the derivation of the uncertainty in κ_{org}, a constant value of 0.64 was used for κ_{inorg}. Combining Eqn. (S9-S11) we have:

$$\kappa_{org} = \frac{1}{x_{org}}\left(\kappa_{CCN} - \kappa_{inorg} \cdot x_{inorg}\right) \quad \text{(S12)}$$

The total volume concentration at the classified size is calculated as:

$$v_{total} = v_{org} + v_{inorg} \quad \text{(S13)}$$

where v_i is the volume concentration of species i. The volume fractions of organics and inorganics are given by:

$$\begin{aligned} x_{org} &= \frac{v_{org}}{v_{total}} = \frac{v_{org}}{v_{org}+v_{inorg}} \\ x_{inorg} &= 1 - x_{org} = \frac{v_{inorg}}{v_{total}} = \frac{v_{inorg}}{v_{org}+v_{inorg}} \end{aligned}, \quad \text{(S14)}$$

Inserting Eq. (S14) into Eq. (S12), we can write the uncertainty in derived κ_{org} as:

$$\sigma_{\kappa_{org}}^2 = \left(\frac{\partial \kappa_{org}}{\partial \kappa_{CCN}}\right)^2 \sigma_{\kappa_{CCN}}^2 + \left(\frac{\partial \kappa_{org}}{\partial v_{org}}\right)^2 \sigma_{v_{org}}^2 + \left(\frac{\partial \kappa_{org}}{\partial v_{inorg}}\right)^2 \sigma_{v_{inorg}}^2 \quad \text{(S15)}$$

where

$$\begin{aligned} &\frac{\partial \kappa_{org}}{\partial \kappa_{CCN}} = \frac{1}{x_{org}} \\ &\frac{\partial \kappa_{org}}{\partial v_{org}} = \frac{\kappa_{CCN} - \kappa_{org}}{v_{org}} \\ &\frac{\partial \kappa_{org}}{\partial v_{inorg}} = \frac{(\kappa_{CCN} - \kappa_{inorg})}{v_{org}} = \frac{(\kappa_{CCN} - \kappa_{inorg})x_{inorg}}{v_{inorg}x_{org}} \end{aligned} \quad \text{(S16)}$$

Substituting Eq. (S16) into (S15) gives:

$$\sigma_{\kappa_{org}}^2 = \left(\frac{\kappa_{CCN}}{x_{org}}\right)^2 \left(\frac{\sigma_{\kappa_{CCN}}}{\kappa_{CCN}}\right)^2 + \left(\kappa_{CCN} - \kappa_{org}\right)^2 \left(\frac{\sigma_{v_{org}}}{v_{org}}\right)^2 + \left(\frac{\kappa_{CCN} - \kappa_{inorg}}{x_{org}} \cdot x_{inorg}\right)^2 \left(\frac{\sigma_{v_{inorg}}}{v_{inorg}}\right)^2 \quad \text{(S17)}$$

From Eqn. (S12), we have:

$$\begin{aligned} \kappa_{CCN} - \kappa_{org} &= \kappa_{inorg}x_{inorg} + \kappa_{org}x_{org} - \kappa_{org} \\ &= \kappa_{inorg}x_{inorg} - \kappa_{org}\left(1 - x_{org}\right) \\ &= \kappa_{inorg}x_{inorg} - \kappa_{org}x_{inorg} \\ &= \left(\kappa_{inorg} - \kappa_{org}\right)x_{inorg} \end{aligned} \quad \text{(S18)}$$

Similarly we have:

$$\begin{aligned}\kappa_{CCN}-\kappa_{inorg} &= \kappa_{org}x_{org}-\kappa_{inorg}\left(1-x_{inorg}\right)\\ &= \kappa_{org}x_{org}-\kappa_{inorg}x_{org}\\ &= -\left(\kappa_{inorg}-\kappa_{org}\right)x_{org}\end{aligned} \quad (S19)$$

Equation (S17) can be simplified by inserting Eqn (S18) and (S19):

$$\begin{aligned}\sigma^2_{\kappa_{org}} &= \left(\frac{\kappa_{CCN}}{x_{org}}\right)^2\left(\frac{\sigma_{\kappa_{CCN}}}{\kappa_{CCN}}\right)^2+\left(\kappa_{inorg}-\kappa_{org}\right)^2 x^2_{inorg}\left(\frac{\sigma_{v_{org}}}{v_{org}}\right)^2+\left(\kappa_{inorg}-\kappa_{org}\right)^2 x^2_{inorg}\left(\frac{\sigma_{v_{inorg}}}{v_{inorg}}\right)^2\\ &= \left(\frac{\kappa_{CCN}}{x_{org}}\right)^2\left(\frac{\sigma_{\kappa_{CCN}}}{\kappa_{CCN}}\right)^2+\left(\kappa_{inorg}-\kappa_{org}\right)^2 x^2_{inorg}\left[\left(\frac{\sigma_{v_{org}}}{v_{org}}\right)^2+\left(\frac{\sigma_{v_{inorg}}}{v_{inorg}}\right)^2\right]\end{aligned} \quad (S20)$$

The first term on the right hand side of Eqn. (S20) is associated with the uncertainty in derived κ_{CCN}. Base on Eq. (4) in the main text, the uncertainty in κ_{CCN} is given by:

$$\begin{aligned}\sigma^2_{\kappa_{CCN}} &= \left(\frac{\partial\kappa_{CCN}}{\partial D_p}\right)^2\sigma^2_{D_p}+\left(\frac{\partial\kappa_{CCN}}{\partial S^*}\right)^2\left(\sigma^2_{S^*}\right)\\ &= \left(\frac{3\kappa_{CCN}}{D_p}\right)^2\sigma^2_{D_p}+\left(\frac{2\kappa_{CCN}}{S^*}\right)^2\left(\sigma^2_{S^*}\right)\end{aligned} \quad (S21)$$

Therefore we can write the relative uncertainty in κ_{CCN} as:

$$\left(\frac{\sigma_{\kappa_{CCN}}}{\kappa_{CCN}}\right)^2 = 9\left(\frac{\sigma_{D_p}}{D_p}\right)^2+4\left(\frac{\sigma_{S^*}}{S^*}\right)^2 \quad (S22)$$

$\frac{\sigma_{D_p}}{D_p}$ represents the accuracy of the dry size of particles classified by the DMA, which is mainly determined by the accuracy of DMA sheath flow rate and classifying voltage, and is typically less than 2% (Wang et al., 2003). As *S** was derived from data collected during periods ranging from 7.6 to 14 hours, the uncertainty of *S** can be attributed to the accuracy in instrument

supersaturation (i.e., uncertainty in calibrated instrument supersaturation), counting statistics, and the potential variation due to minor changes in particle composition during the periods. The uncertainty in calibrated instrument supersaturation was estimated from the uncertainty of the dry size of pure ammonium sulfate particles classified by DMA during calibration and the standard deviation of the repeated calibrations performed before and after the field study, and this uncertainty was generally less than 2% (relative uncertainty). The uncertainty due to counting statistics and potential variations in particle composition during the periods combined was estimated from the standard error (standard deviation divided by the square root of the sample number) of S^* derived from multiple measurements during the periods, and ranged from 2% to 5%, which dominated the uncertainty in derived S^* and the overall uncertainty in κ_{CCN}. The overall uncertainty in derived κ_{CCN} ranged from 5% to 12%.

The second term on the right hand side of Eqn. (S20) represents contributions due to the uncertainties in volume fractions of organics and inorganics (i.e. particle composition). The volume fractions were derived from the average mass concentrations measured during the periods, and densities of the species. For sulfate and nitrate, the uncertainty in their densities should be negligible. The organic density estimated from O:C (ranged from 0.29 to 0.46) and H:C (ranged from 1.49 to 1.28) ratios ranged from 1150 to 1350 kg m^{-3} (Kuwata et al., 2012). The assumed organic density of 1250 kg m^{-3} represented an uncertainty less than 8%, which was significantly smaller than the uncertainty in measured organics mass concentration. As shown later, only periods that showed minimum variation in particle composition were selected for the analysis, therefore, the minor variation of particle composition during these periods was neglected, and the uncertainty in volume fractions for these periods were estimated from the uncertainty of mass concentration measurements measured by AMS. The uncertainties in mass

concentrations measured by AMS were generally ~30% (Middlebrook et al., 2012) . However, it is worth noting that not all uncertainties in measured mass concentrations translate into uncertainty in derived species volume fractions. For example, one major uncertainty in mass concentrations measured by AMS originates from the uncertainty in collection efficiency (i.e., particle bounce). However, for internally mixed particles observed at T1 site, the collection efficiency influenced measured mass concentrations of both non-refractory inorganic and organic components to the same degree, and therefore had little impact on the derived volume fractions of the components. For the purpose of estimating uncertainty in species volume fraction, an uncertainty of 10% was estimated for measured inorganics and organics mass concentrations, which were mainly due to the uncertainties in relative ionization efficiencies.

References

Bougiatioti, A., et al.: Size-resolved CCN distributions and activation kinetics of aged continental and marine aerosol, Atmos. Chem. Phys., 11, 8791-8808, doi: 10.5194/acp-11-8791-2011 2011.

Cerully, K. M., et al.: Aerosol hygroscopicity and CCN activation kinetics in a boreal forest environment during the 2007 EUCAARI campaign, Atmos. Chem. Phys., 11, 12369-12386, doi: 10.5194/acp-11-12369-2011, 2011.

Kuwata, M., Zorn, S. R., and Martin, S. T.: Using Elemental Ratios to Predict the Density of Organic Material Composed of Carbon, Hydrogen, and Oxygen, Environ. Sci. Technol., 46, 787-794, 2012.

Lance, S.: Quantifying compositional impacts of ambient aerosol on cloud droplet formation, Ph.D., Georgia Institute of Technology, Atlanta, 2007.

Lance, S., et al.: Aerosol mixing-state, hygroscopic growth and cloud activation efficiency during MIRAGE 2006, Atmos. Chem. Phys. Discuss., 12, 15709-15742, doi:10.5194/acpd-12-15709-2012, 2012.

Mei, F., et al.: Droplet activation properties of organic aerosols observed at an urban site during CalNex-LA, J. Geophys. Res., In Press, 2012.

Middlebrook, A. M., Bahreini, R., Jimenez, J. L., and Canagaratna, M. R.: Evaluation of Composition-Dependent Collection Efficiencies for the Aerodyne Aerosol Mass Spectrometer using Field Data, Aerosol Sci. Technol., 46, 258-271, 2012.

Padro, L. T., et al.: Mixing state and compositional effects on CCN activity and droplet growth kinetics of size-resolved CCN in an urban environment, Atmos. Chem. Phys., 12, 10239-10255, doi:10.5194/acp-12-10239-2012, 2012.

Wang, J., Flagan, R. C., and Seinfeld, J. H.: A differential mobility analyzer (DMA) system for submicron aerosol measurements at ambient relative humidity, Aerosol Sci. Technol., 37, 46-52, 2003.